Evolution, 2023, **77(12)**, 2619–2630
https://doi.org/10.1093/evolut/qpad174
Advance access publication 5 October 2023
Original Article

Early origin and diverse phenotypic implementation of iridescent UV patterns for sexual signaling in pierid butterflies

Vincent Ficarrotta[1,2], Arnaud Martin[1] Brian A. Counterman[2], R. Alexander Pyron[1]

[1]Department of Biological Sciences, The George Washington University, Washington, DC, United States
[2]Department of Biological Sciences, Auburn University, Auburn, AL, United States

Corresponding author: Department of Biological Sciences, The George Washington University, Washington, 800 22nd St NW Ste 2885, DC 20052, United States. Email: vficarrotta@gmail.com

Abstract

Iridescent ultraviolet (IUV) patterns on pierid butterfly wings are phenotypic adaptations commonly used as sexual signals, generated by scales with ultrastructural modifications. Pierid IUV patterns are sexually dichromatic, with reduced size in females, where conspicuous sexual signaling balances courtship against ecological predation. There have been no phylogenetic reconstructions of IUV within Pieridae and little morphological characterization of phenotypic diversity. Our genus-wide characterization of IUV revealed the uniform similarity of stacked lamellar ridges on the dorsal surface of cover scales. We tested a hypothesis of single versus multiple origins by reconstructing a phylogeny of 534 species (~43.2% described species), with all genera represented, and a trait matrix of 734 species (~59.4%) screened for IUV. A single, early dimorphic origin of IUV followed by several losses and gains received strong support, concluding that IUV patterns and structural coloration are old traits. Collectively, these results support the homology of IUV scales and patterns that diversified within several lineages, suggesting an interplay between female-mediated sexual selection and ecological predatory selection.

Keywords: ultraviolet, butterflies, ancestral state reconstruction, morphological evolution, sexual dichromatism, sexual signaling

Introduction

The butterfly family Pieridae contains ~1,235 described species, known for displays of yellows, oranges, reds, and black and white (Descimon, 1975; van der Bijl et al., 2020), Spectacularly, some species also display iridescent, ultraviolet (IUV) patterns (Ghiradella, 1984; Ghiradella et al., 1972; Hirata & Kubota, 1957; Kemp & Rutowski, 2007; Nekrutenko, 1965; Silberglied & Taylor, 1973; Wilts et al., 2011). Previous studies have shown the sexual signaling function of IUV in both inter- and intraspecific courting events of several Coliadinae species (Kemp, 2008; Kemp & Rutowski, 2011; Silberglied & Taylor, 1978; Stella & Kleisner, 2022). Conspicuous male sexual ornamentation evolution balances female-mediated sexual pressures and predatory ecological pressure (Fisher, 1915; Holmes et al., 1979), where birds (Cuthill et al., 2000), reptiles (Osorio, 2019), and other insects can detect UV (Chittka & Menzel, 1992; van der Kooi et al., 2021). Additionally, IUV ornamentation covaries strongly with climate and geography (Pecháček et al., 2014, 2019; Stella et al., 2018; Stella et al., 2018), suggesting multilevel and patterns of natural and sexual selection (Brunton, 1998).

Little is known about the evolutionary origin of pierid IUV, including the ancestral state, number of origins, rates of transition between states (presence and absence in males and females or both sexes), and potential reversals of states. Previous phylogenetic studies of IUV ornamentation among Coliadinae support a history of sexual selection influencing both IUV and speciation (Brunton & Majerus, 1995; Kemp et al., 2005). Gains and losses of IUV stem from the complex interplay between ecological and sexual selection in recent radiations, a phenomenon that may be facilitated by the simple genetic basis of IUV variation as shown in *Colias* hybrid zones (Ficarrotta et al., 2022). Despite the importance of IUV in Pieridae diversification, there have been no attempts to reconstruct the evolutionary origins of IUV or assess the homology of IUV across pierid butterflies since Brunton (1998) wherein only a handful of genera were analyzed. Such estimates are needed to construct and address hypotheses that untangle the relative roles of mate choice and ecology.

Lepidopteran scales are the units of wing color patterns and develop as a bilayer of cover and ground scales (Dinwiddie et al., 2014). IUV is a structurally based color generated by ultrastructures on the upper laminal scale surface (Ghiradella et al., 1972; Silberglied & Taylor, 1973; Wijnen et al., 2007; Wilts et al., 2011). These ultrastructures are characterized as stacks of tightly packed, flanged cuticle ridges (Ghiradella, 1974; Ghiradella et al., 1972) and are visible when scale cross-sections are imaged (Ghiradella, 1984; Ghiradella et al., 1972). The lamellar ridges of ultrastructures develop at a higher density than noniridescent reflecting ground scales and include between 6 and 12 stacked layers depending on the species (Ghiradella, 1974; Wilts et al., 2011). Pterin pigments, which reflect white, yellow, orange, and red hues (Watt, 1964, 1967), also absorb ultraviolet wavelengths (Wilts et al., 2011).

Received June 22, 2023; revisions received September 1, 2023; accepted October 4, 2023
Associate Editor: Susanne Foitzik; Handling Editor: Miriam Zelditch

Pterins enhance the spectral purity of IUV reflectance. They absorb scattered ultraviolet wavelengths passing through the upper lamina (Rutowski, 1985; Rutowski et al., 2005; Wilts et al., 2011), leaving only the iridized UV wavelengths reflected by the ultrastructures. Imaged IUV wing patterns revealed that IUV patterns can be fairly common depending on the genus yet variable in size, often including major differences between sexes and closely related species (Pecháček et al., 2014; Stella et al., 2018). Despite the prevalence and diversity of IUV among Pieridae, it remains unknown if homologous scale morphologies are responsible for the diversity of IUV reflection and patterns across the phylogeny.

The evolutionary history of sexual dichromatism can be complex, sometimes originating once with subsequent losses and atavistic gains or, conversely, the sexual trait may evolve multiple times independently (Blaimer et al., 2018; Hendry et al., 2014; van der Bijl et al., 2020) in a scenario of convergent evolution. Here, we use two approaches for studying the homology of IUV scales in Pieridae. First, we image the scales of 11 specimens representing their genera from the total of 17 genera with IUV patterns. Ridge density measurements of cover and ground scales are shown to be unmistakably exaggerated in IUV patterns across all 11 species. Additionally, IUV pattern spectral reflectance data of the 11 specimens (spectrophotometer methods in Supplementary Methods section) is plotted and is consistent with previous studies recording reflectance spectra of IUV patterns (Kemp & Rutowski, 2007). Second, we produce a time-calibrated multilocus phylogeny of 534 pierid species (43.2% of species and 99.9% of genera) complementing a trait matrix of 734 species (59.4% of species and 99.9% of genera) scored for presence–absence of IUV for both sexes from museum IUV pattern screenings. Using the intersecting data set of 375 taxa (30.4% of species and 99.8% of genera), we compared 60 models of ancestral state reconstructions. The various models included equal or variable transition rate parameters, hidden rates, and a priori hypotheses for ancestral states at several major nodes.

We ask whether the IUV trait observed across multiple subfamilies of Pieridae is homologous by assessing the similarity of wing-scale structural morphology and estimating ancestral states to estimate support for single versus multiple origins. Specifically, we hypothesize that the phenotypic expression of IUV originated once early in Pieridae, and has been repeatedly lost and gained, likely due to the complex interplay between ecological and sexual selection. This evolutionary pattern may be facilitated by the simple genetic basis of IUV variation as seen in *Colias* (Ficarrotta et al., 2022) and stands opposite of multiple origins of IUV where similarly reflecting scales would convergently evolve. Then, we corroborate the phenotypic observations with the evolutionary model-fitting using our phylogenetic estimations.

Methods

Tree construction

Major advances have recently resolved the phylogenetic relationships of butterfly families (Espeland et al., 2018; Wiemers et al., 2020). Although these provided insights into relationships among subfamilies of Pierinae (Edger et al., 2015; Espeland et al., 2018; Wahlberg et al., 2014), they do not offer species-level resolution. Fortunately, sequence data from previous pierid experiments are available in public repositories (Edger et al., 2015; Espeland et al., 2018; Hill et al., 2019; Nazari et al., 2011; Wahlberg et al., 2014) suitable for phylogenetic analysis. Previous studies agree Pieridae contains four subfamilies with dramatically unequal species richness: Pseudopontiinae (6 species, 0.5%), Dismorphiinae (69, 5.6%), Coliadinae (223, 18.1%), and Pierinae (937, 75.9%), where IUV is restricted to Coliadinae and Pierinae.

We constructed a species-level tree from the sequence data of previous studies stored on GenBank (Dapporto et al., 2017; Dincă et al., 2011; Ding & Zhang, 2017; Heidel-Fischer et al., 2010; Nazari et al., 2011) and the iBOL database, which makes for a suitable supermatrix analysis. (Dequeiroz & Gatesy, 2007). We used the method PyPHLAWD (Smith & Walker, 2019), a fully automated, partially supervised construction of a supermatrix for a given taxon Steps included generating a local database and performing a preliminary run of PyPHLAWD under the default clustering and assembly settings, which also included FastTree (Price et al., 2010) a preliminary gene-tree generator useful for screening and trimming outliers. This initial alignment consisted of 23 clusters, 683 taxa (including subspecies), and 23,069 bp. Custom R scripts were then used to identify minor groups, redundant subspecies, and nonspecific taxa, which were excluded and can be found in the Dryad repository: DOI: 10.5061/dryad.8931zcrx3. PyPHLAWD was reran, which produced an initial supermatrix alignment of 23 clusters, 531 species, and 21,592 bp, which is 2.6 times larger than the previous supertree of Hill et al., 2019. The following outgroups were added to the alignment: Papilionidae: *Papilio glaucus*, Hesperiidae: *Hasora chromus*, Hedylidae: *Macrosoma tipulata*, Nymphalidae: *Danaus plexippus*, Riodinidae: *Riodina lysippus*, and Lycaenidae: *Lycaena alciphron*. The full list of species names, NCBI Taxonomy IDs, and GenBank accession numbers is given in the Dryad repository. The final matrix has 23 clusters, 537 taxa, and 26,240 bp, and is 19.6% complete overall.

The final matrix was analyzed in RAxMLv8.2.12 0 (Stamatakis, 2014), with a GTRGAMMA model applied to each partition, 1,000 rapid-bootstrap replicates, 200 ML searches from every fifth replicate, and a final ML optimization to infer a phylogeny. To avoid arifactually inaccurate bootstrap values (McMahon & Sanderson, 2006; Simmons & Goloboff, 2014), we performed an additional search in RAxML to estimate the NNI-optimal tree. Support was calculated using the SH-like aLRT statistic (Anisimova & Gascuel, 2006), which is shown to result in higher precision and accuracy of SHL over bootstrap for sparse supermatrices (Anisimova & Gascuel, 2006; Pyron & Wiens, 2011) and though authors note the need for caution in interpreting support values for analyses that do not thoroughly assess branch support across all characters (Simmons & Goloboff, 2014), they nonetheless found that SHL values are generally reliable for identifying poorly supported clades. Following previous recommendations (Pyron & Wiens, 2011), we interpret SHL > 84 to represent "strong" support.

Temporal calibration

We mapped the resulting tree from our large-scale supermatrix to this chronogram using the "congruify" package in R (Eastman et al., 2013), which matches the congruent nodes between a dated reference tree and an undated target tree using the treePL algorithm (Smith & O'Meara, 2012) to calibrate the target tree. One remaining rogue taxon (*Catasticta semiramis*) was trimmed from the dated phylogeny. The

resulting time-calibrated tree (Pieridae_treePL_trim.tre) is highly congruent with existing pierid chronograms (Edger et al., 2015; Espeland et al., 2018; Hill et al., 2019; Wahlberg et al., 2014) and is therefore amenable to downstream analyses, particularly ancestral state estimation and rates of character evolution.

SEM sample preparation and imaging: wing tissue

Wing tissue with IUV patterns was cut and attached to an SEM stub using a thin layer of silver paste adhesive. Samples were left to dry overnight and then sputter coated with gold using a Cressington 208HR Sputter Coater. The first round applied 12 nm of gold to the top surface of the wing tissue and the second round applied 7 nm at a 45° angle. Images were acquired on an FEI Teneo LV SEM with the following parameters: 2.00 kV, 25 pA, and dwell time of 10 µs with detection performed by the Everhart–Thornley detector. Modifications for imaging cross-sections are in Supplementary Methods.

Temporal calibration

The IUV wing patterns of pierid butterflies were first noted in the Common Brimstone (*Gonepteryx rahmni*) (Coliadinae) by Mazokhin-Porshnyakov (Mazokhin-Porshnyakov, 1954), with later imaging revealing the pattern and describing the sexually dimorphic trait (Nekrutenko, 1965). Some species (*Colias aurora* and Queen Purple Tip [*Colotis regina*]) (Wilts et al., 2011) display an iridescent purple sheen where IUV patterns exist, likely due to the same morphology producing IUV, and was perhaps the only clue that IUV reflection existed prior to its discovery. Now, IUV is described in a handful of genera including *Colias* (Hirata & Kubota, 1957; Silberglied & Taylor, 1973), *Gonepteryx* (Nekrutenko, 1965), *Phoebis*, *Aphrissa*, and *Kricogonia* (Allyn & Downey, 1977), *Eurema* (Ghiradella et al., 1972), *Zerene* (Brunton & Majerus, 1995; Fenner et al., 2019), *Afrodryas leda* (formerly *Eronia leda*) and *Colotis* (Stavenga et al., 2006; Wijnen et al., 2007), *Eroessa* (Ingram & Parker, 2008), *Anteos* (Rutowski et al., 2007), and *Hebomoia* (Shur et al., 2017). Our IUV screening performed at the National Museum of Natural History and the McGuire Center for Lepidoptera & Biodiversity led to the discovery of three additional genera with IUV patterns (*Dercas*, *Ixias*, and *Zegris*). Certain specimens were carefully imaged in the visible and UV ranges, and the plates are in Supplemental Material Plates 1–5 and *Colias* Plates 1–13.

Ultraviolet microphotography

Close-up views of IUV scales were imaged at a magnification of ~10.25X. See supplemental materials for the full list of imaging parts. Briefly, a highly modified Panasonic G3 camera with multiple filters allowed for the acquisition of ultraviolet-wavelength images in black and white. Illumination was provided by a combination of GE Blacklights 13-Watt T3 Spiral Light Bulbs and a Convoy S2 365nm LED torchlight. Stacks of 50–100 images were taken using a Stackshot focusing rail at ISO 400 and shutter speeds of 1/2.5–1/3.2 s, and deconvolved using the Depth Map method in the Helicon Focus software. UV images were overlaid to visible range images taken with a Keyence VHX-5000 digital microscope, using Photoshop, and the Warp tool for aligning layers while accommodating minor differences in angle of acquisition and lens features. These overlays are shown with individual layers and with the output of the "Lighten" layer blending mode in Photoshop.

Measuring ridge density and statistical analysis

To investigate morphological similarity, we compared the lamellar ridge density across the upper surface of cover and ground scales from IUV patterns across 11 representative species specimens from genera with IUV species. Ridges run longitudinally across the upper laminal scale surface, with noticeable differences between scale types. Scale top views were imaged at 2,000× magnification using the SEM and measured in Photoshop, with average ridge distances measured across intervals of 10 ridges. Ten scales of both cover and ground from 11 specimens were measured, and ridge density was calculated by dividing the number of ridges (10) by the length of the drawn line. An ANOVA tested for a significant difference between the ridge density of cover and ground scales using a random-effects model to compensate for the nonindependence of species measurements due to phylogenetic structuring. Analyses were performed using the following R packages: *lme4* (Bates et al., 2015), *dplyr* (Wickham et al., 2022), and *rapportools* (Blagotić & Daróczi, 2022).

Ancestral state reconstruction

We hypothesized a single evolutionary origin of IUV if it is indeed homologous and to do this we tested early algorithms for estimating ancestral states (Pagel, 1994; Schluter et al., 1997) and also more recent hidden rates models (Beaulieu et al., 2013; Smith et al., 2010) that are expected to better reflect the complex evolutionary dynamics underlying a character such as mutual ornamentation. These recent methods attempt to address complexity by including "hidden" states, where the dynamics of gains and losses can vary in different parts of the tree while also considering correlated characters. Our two binary characters are the presence and absence of dorsal IUV reflectance in males and females, respectively. Female ultraviolet presence is never observed with male absence, and thus all rates and states associated with male absence/female presence (0/1) can be excluded from the state space. Of all species screened, 129 of 734 displayed IUV (17.6%) and 70 of 734 displayed mutual IUV (1%), or IUV in both sexes. All analyses were performed in the R package "corHMM" (Beaulieu et al., 2017).

We used the correlated binary HMM models to account for the potential presence of multiple hidden-rate categories across IUV presence and absence in males and females. Thus, IUV is a discrete trait of presence or absence and is in coded three different ways. First, the presence–absence of all instances of IUV per species were modeled under Mk1 and Mk2 rate matrices, allowing for transitions between states to be of equal or different rates, respectively. Second, binary coding was modeled under Mk1 and Mk2 as well (i.e., Pagel, 1994). Binary coding is used to differentiate between the presence and absence of each sex. A male-only IUV binary is scored as (1,0) whereas both male and female are scored as (1,1). Third, a multistate coding was modeled again under Mk1 and Mk2 conditions while incorporating sexual dimorphism by scoring absence as 0, presence in males as 1, and presence in both sexes as 2. For these three coding methods, a model was generated that included no hidden rates, one hidden rates or two hidden rates. From all considered models, two models were chosen to represent the ancestral state reconstructions: under all instances of IUV and under sex-specific IUV data. Models were compared using AICw, with strong (>0.9) and moderate (<0.9) support evaluated for competing models.

Using the first coding method, we examined the presence or absence of IUV where we fit ER and ARD models without hidden rate categories. We then used a hidden-rate category allowing for two sets of gain/loss rates (ARD2) (Beaulieu et al., 2013). We also implemented a symmetrical, 4-parameter version of this model with one bidirectional transition rate between each pair of states and rates (ER2). We did not fix the root state for these hidden-rate models, as this would necessitate choosing a rate class a priori. Instead, we used the *root.p="yang"* option to employ the conditional strategy of Yang (2006) as recommended by J.M. Beaulieu (personal communication).

We compared two sets of models to evaluate the evolutionary dynamics of IUV per sex (see Pagel, 1994) using the second (binary) and third (multistate) coding methods and fit standard ER, SYM, and ARD models. Second, we used the approach of Smith et al. (2010), fitting ER, SYM, and ARD models to a restricted state space of the co-occurrence of these two binary traits and disallowing simultaneous changes. The primary difference between these two model sets is whether state changes are constrained to pass through intermediate (male-only) states or not.

Finally, the node joining Coliadinae and Pierinae (third node) was fixed for each state of absence, male-only presence, and both presences. The node constraints were applied to all previous parameter combinations for a total of 60 tested models. The following packages developed for R (R Core Team, 2022) were also used: *ape* (Paradis & Schliep, 2019), *phytools* (Revell, 2012), and *geiger* (Pennell et al., 2014).

Supplementary Methods section includes spectrophotometry, scale cross-section mounting for SEM, description of scoring IUV in museum specimens, and extended explanations of phylogenetic analysis, ancestral state reconstructions, and microphotography.

Results

Phylogeny

To generate a taxon-rich phylogeny of Pieridae, we used PyPHLAWD (Smith & Walker, 2019) to compile a supermatrix of available pierid sequences and computed a dated ML supertree encompassing 534 species (Figure 1). Overall, 55% of nodes are strongly supported (SHL > 85). Some genera such as *Phoebis*, *Eurema*, *Appias*, *Aporia*, *Pieris*, *Catasticta*, and *Euchloe* appear non-monophyletic as in previous studies (Edger et al., 2015; Wahlberg et al., 2014). Similarly, the timescale of the tree is fixed at higher levels than that of Hill et al. (2019) and is thus congruent with several previous time-calibrated analyses (Edger et al., 2015; Espeland et al., 2018; Hill et al., 2019), with a late Cretaceous origin of Pieridae (~86 Ma), and subsequent Cenozoic diversification in the most diverse groups.

The resulting topology is broadly concordant with most recent studies (e.g., Hill et al., 2019; Wahlberg et al., 2014; Wiemers et al., 2020), notably supporting the positioning of the *triba nova* Leptosiaini and Nepheroniini (Wahlberg et al., 2014) at the base of Pierinae. Unlike previous studies, our reconstruction positions the genus *Elodina* at the base of the Pierini tribe (58.2 SHL) rather than included in the polytomous node at the base of Pierinae (Edger et al., 2015; Wahlberg et al., 2014). Finally, we find support for the previously proposed monophyly of the rogue *Afrodryas* genus (Nazari et al., 2011), with a single extant species (*Afrodryas leda* [autumn leaf vagrant], formerly *Eronia leda*) positioned at the base of Pierinae. While our reconstruction places Afrodryas outside of any proposed tribe, we note that the recent phylogeny (Kawahara et al., 2023) proposes its placement within Teracolini albeit without node support scores available. Overall, given the general congruence with the most recent estimates of pierid phylogeny and divergence times, we believe this topology and timescale represent a robust basis for downstream phylogenetic comparative analyses. Of the 734 screened species and the 534 species in the phylogeny, 375 were present in both data sets. Thus, we pruned the tree branches with missing data to this set of 375 species for the model-fitting analyses described above without loss of analytical power (Supplementary Figure 2). All further descriptions of model results refer to this reduced data set.

IUV scale imaging, scale ultrastructure analysis, and reflective spectral analysis

SEM images of IUV scales show consistency in morphology across multiple IUV genera from both a wing surface view and when cross-sectioned (Figure 2A). Additionally, IUV scales only occupy the cover layer, indicating an underlying genetic identifier between the ground and cover scales during development (Figures 2A and 3). The IUV scales display increased numbers of lamellar ridges running longitudinally across the scale, and an ANOVA performed on the ridge density between IUV cover and ground scales (F = 1651.9, total df = 219, p-value = 2.2e-16) demonstrates the strength in morphologic deviation from each other due to the IUV ultrastructures. A random-effects linear mixed model was employed to compensate for the nonrandom, phylogenetic structure of organisms, which was used to calculate the ANOVA using the *lme4* R package (Bates et al., 2015). Interspecific comparisons of ridge density calculations (Figure 2B) in conjunction with SEM images (Figure 2A) also reveal a uniformity in ground-scale phenotype and a higher level of conservation compared to the variation in cover scales. High-magnification ultraviolet photography demonstrates the angle-dependent band of reflection from IUV scales and the similarity of the reflection among all species (Figure 3), whereas SEM images and measurements display intergeneric variation (Figure 2A). The width and height differences of stacked ridges are observable, for example, the cross-section of *Colotis danae* appears broadest, though the *Hebomoia glaucippe* cross-section includes a similar reinforced structuring of stacked ridges that is lacking from the cross-sections of *Dercas verhuelli* and *Zegris fausti*.

Evolutionary models

The model "binary.ER.f3" is highly supported (AICcw = 0.93) of the mutual models considering sex-specific scoring of IUV (Table 1, Supplementary Table 3) and estimates a single origin of IUV at the root of Pieridae (Figure 4) and best explains the evolutionary trajectory of IUV and the polyphyletic mapping of IUV as a trait in the phylogeny. A single origin of IUV is strongly supported and suggests that IUV is homologous, which contrasts with a scenario of multiple independent origins that would suggest convergent evolution of scale structure and reflection occurred. The "binary.ER.f3" model used binary data scoring and fixed the joining node of Coliadinae and Pieridae with a trait score of presence in both males and females. Parameter estimates suggest equiprobable gains and losses between states (Table 2), a result possibly

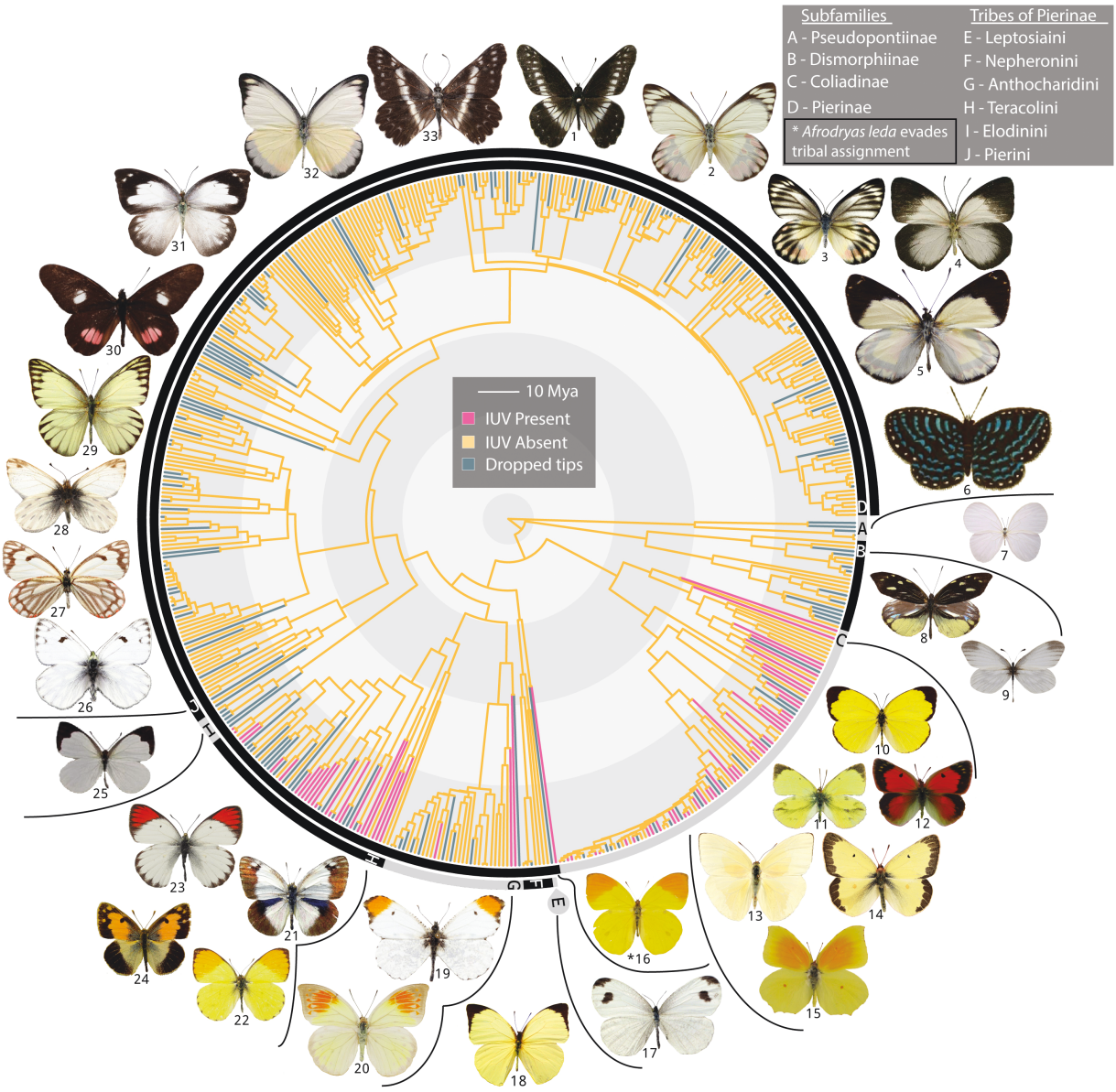

Figure 1. Dated phylogenetic reconstruction of Pieridae includes tip states. Time-calibrated multilocus phylogeny of 534 pierid species, estimated using RAxMLv8.2.12 from a supermatrix of 23 clusters, 537 taxa, and up to 26,240 bp of sequence data per species. The timescale (indicated by contrasting inner rings of 20 Ma) was estimated using the treePL algorithm in congruify, matched to the timetree of Hill et al. (2019). Terminal branches colored pink and orange display the presence and absence of IUV, respectively; those in dark cyan lacked IUV data and were pruned for downstream analyses. Numbers under butterflies correspond to species names in Supplemental Table 4. **Afrodryas leda* (16) is not assigned to a tribe.

reflecting the genetic modularity of IUV elements. Mutually ornamented lineages show high rates of reversal back to both male-only ornamentation, including soon after the origin, and to a total loss of UV reflectance. In conjunction with the morphological analyses, we build a strong case for the homology of IUV in Pieridae. The deep evolutionary origin of IUV patterns suggests that IUV patterns are deeply ingrained in pierid natural history and, as a corollary, structural coloration is an old evolutionary method of butterfly coloration.

We note that no strong support was found when analyzing the 12 models considering the presence and absence of IUV per species, which suggests that this data set lacks the ability to sufficiently estimate a highly supported evolutionary trajectory (Supplementary Table 1). The highest scoring model (ER2; AICcW = 0.44) is a symmetrical model containing two rate classes (an additional hidden rate) with equivalent transitions between states and among classes (Supplementary Figure 1). As in the original paper (Beaulieu et al., 2013), we interpret these hidden rate categories as "slow" and "fast," yielding high and low rates of gains and losses (Supplementary Table 2). The evolutionary dynamics are too complex (e.g., within *Colias*) to be captured adequately with these secondary sets of models and the presence–absence data set and the rates are thus estimated to be arbitrarily high, with uncertain ancestral states in these clades. Therefore, we report these results and describe the analyses but ultimately conclude the analyses in the previous paragraph as informative to the evolutionary dynamics and origins of the IUV.

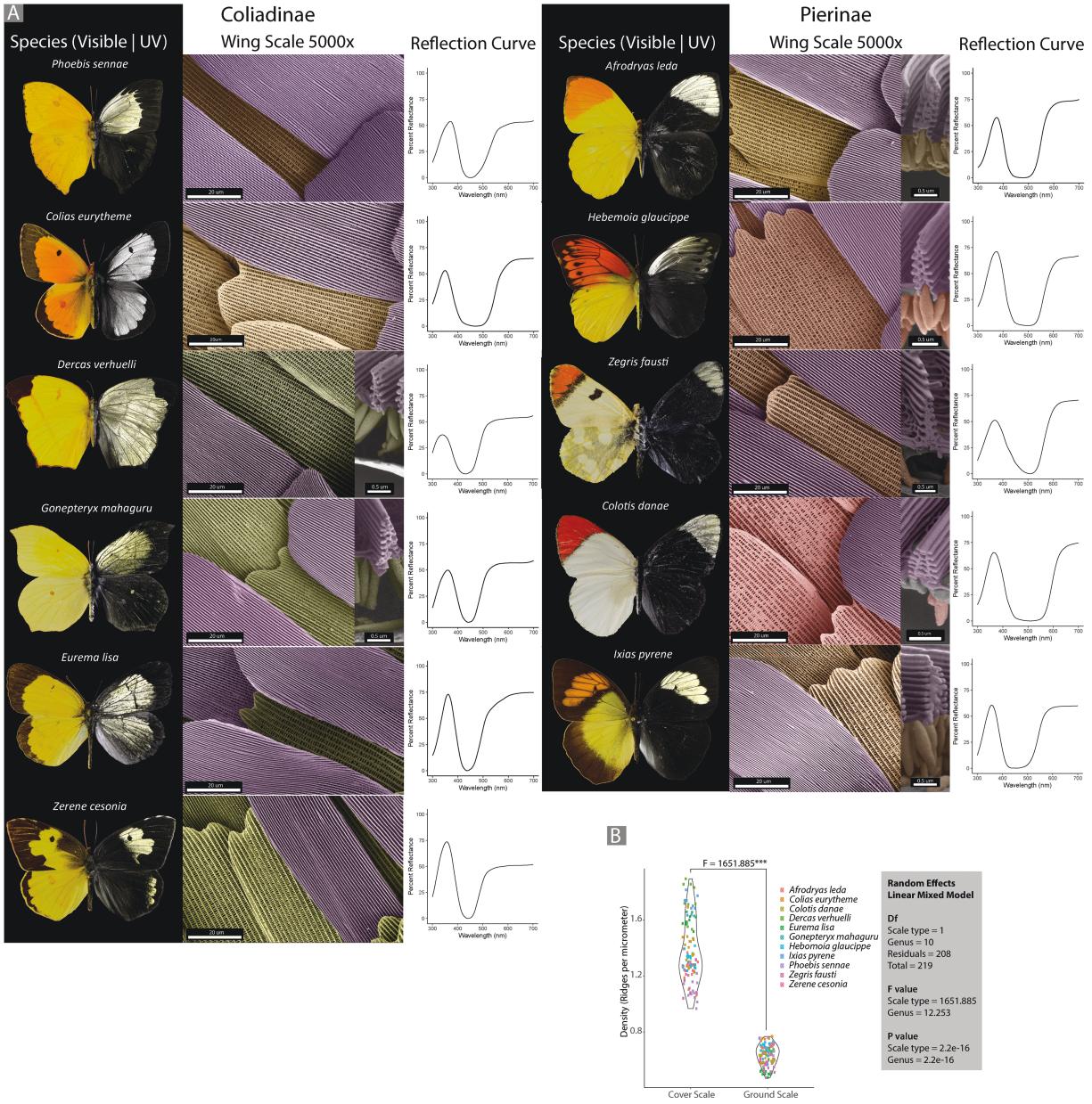

Figure 2. SEM images of IUV cover scales between 11 representative species suggest homology, and an ANOVA of ridge density between cover and ground scales shows consistent and unmistakable differences (F = 1651.885, total df = 219, p-value=2.2e-16). (A) Species were chosen from 11 of the 17 genera with IUV reflecting species as representatives of their genera. The first column shows the species photographed in visible (left) and ultraviolet (right) ranges. The second column shows cover-ground scale morphological differences at 5,000× magnification with inset cross-sections of IUV cover scales displaying the flanged stacks of lamellae that reflect iridized wavelengths. The third column shows the reflectance spectra of IUV pattern elements. (B) Comparison of ridge density between cover and ground scales across 11 IUV species from different genera using a random-effects linear model that accounts for phylogenetic structure. ANOVA produced an F-score of 1651.9.

Discussion

IUV cover scale functional morphology

The intricate ultrastructure of IUV cover scales is conspicuous, using SEM technology allowing us to conclude here that IUV scales occupy the cover scale layer in the wing-scale bilayer, and they display a high degree of interspecific variation though they appear to develop similarly across all species. Ground scales were expected to vary between species in the absence of strong selective pressures to maintain a specific morphology. However, the SEM images and ridge density calculations show strong conservation in morphology across species and genera. High levels of variation in the IUV sexual ornamental scales are consistent with sexual selection theory (Andersson & Iwasa, 1996; Cotton et al., 2004; Radwan, 2008), which describes sexual ornament trait variation as a necessary factor that female preferences act upon. Sexual traits typically have higher responsiveness than nonsexual traits to internal and external factors during development (Lee et al., 2014; Ohlsson et al., 2002) and, indeed, IUV scale responsiveness to diet and abiotic conditions has been demonstrated in previous studies (Fenner et al., 2019; Kemp & Rutowski, 2007). Thus, our observed interspecific variations on IUV scales are consistent with previous literature on the variability of secondary sexual traits in males that are strongly mediated by ecological

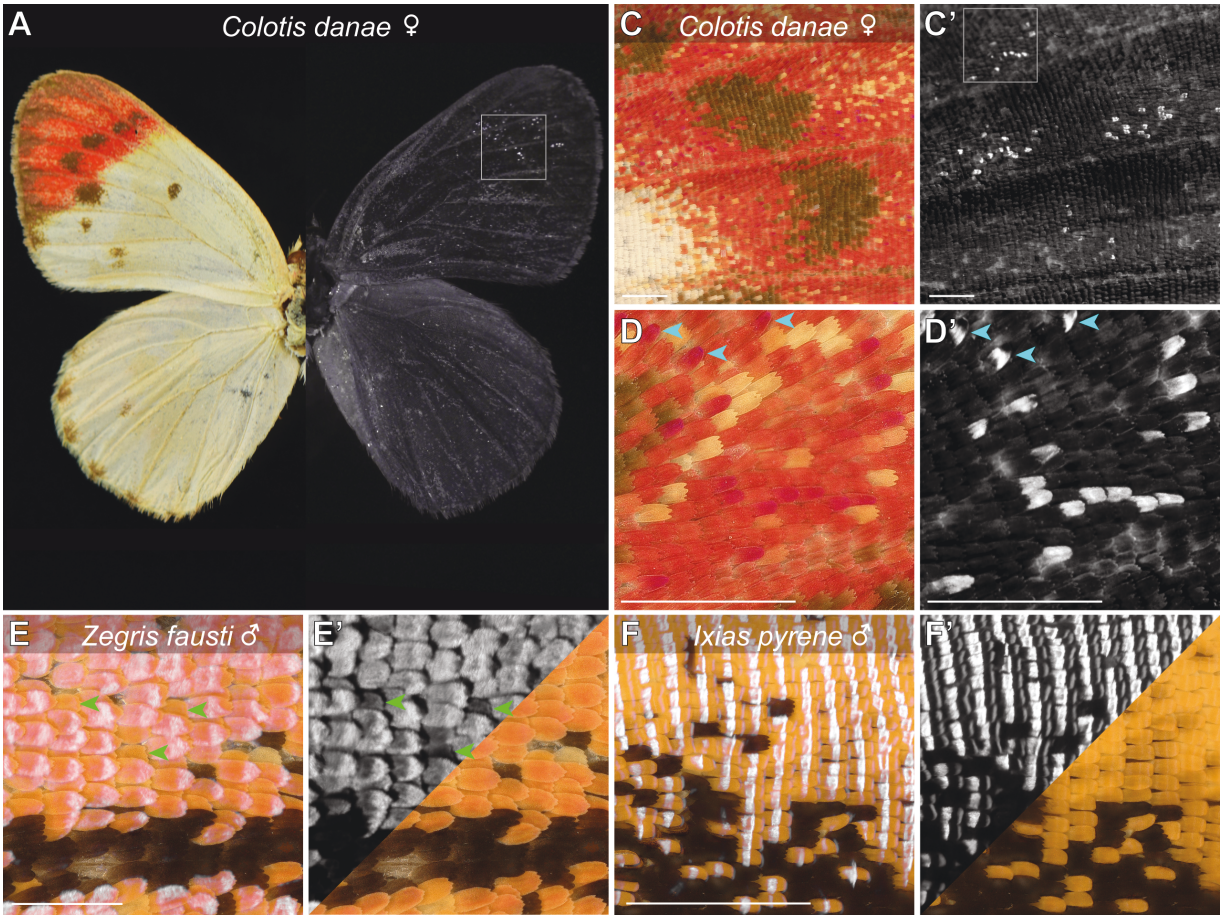

Figure 3. IUV scales are cover scales and can exist in a dispersed state. (A–D') Visible (A, C, D) and ultraviolet (A', C', D') imaging of sparsely distributed IUV scales in the dorsal forewings of *Colotis danae* females. These IUV scales can be confused with UV-reflective wing wear and dust when observed in the far field and require microphotography for proper detection. IUV scale (cyan arrows) shows a round tip and a slightly purple coloration compared to the other red scales of the distal forewing patch. (E–E') Overlaid (E) and split-channel (E') UV-A and visible microphotographs of a dorsal forewing IUV patch in a *Zegris fausti* male. Ground scales are orange pigmented and lack IUV (green arrows). (F–F') In *Ixias pyrene* male dorsal wings, cover scales are black and completely covered by IUV scales. IUV scales are highly reflective and produce curvature-dependent stripes of signal when illuminated at most angles of incidence. Scales bars: 500 μm.

Table 1. Model-fitting results for mutual ornamentation preferred binary. ER.f3 (0.93 AICw). ER = equal rates, ARD = All Rates Different, SYM = symmetrical rates, F1 = third node (Pierinae/Coliadinae split) fixed for absence, F2 = third node fixed for male-only presence, F3 = third node fixed for presence in both sexes. The strongly preferred model (in bold text) uses binary coding and equal rates, with the third node set to present for mutual ornamentation.

Models	loglik	AIC	AICc	AICw
binary.ER.F1	−242.8179	487.6357	−242.8179	0.02
binary.ER.F2	−245.3416	492.6833	−245.3416	0.06
binary.ER.F3	**−250.9772**	**503.9545**	**−250.9772**	**0.93**

and environmental factors (Pecháček et al., 2014; Pecháček et al., 2019; Stella et al., 2018).

Female preference for IUV reflection also depends on the receptive sensitivity of their opsins. The wavelengths reflected by the scales are mediated by the spacing of the flanged stacks of lamellar ridges (i.e., branches on a Christmas tree) (Ghiradella et al., 1972). When developmental parameters change, optical effects can be modified (e.g., the purple sheen noted earlier). With the need for consistent morphology to reflect within the female-perceived ultraviolet-wavelength ranges, variation in brightness, as opposed to shifts in the reflectance peak, makes sense in the context of female visual sensitivity. The brightness of IUV reflection can signal useful information to females, such as the male's age (Rutowski, 1985); however, a male reflecting a hue outside the perceptive capabilities of the female cannot be detected. Our data show clustering of ridge density by species (Figure 2B) as well as differences in certain parts of the ultrastructures between species (Figure 2A), which is potentially species-specific tuning or adaptations of the sending and receiving parameters of the sexual signal. We theorize that the ultraviolet reflectance peak of IUV scales should correlate with the absorbance peak of ultraviolet-sensitive photoreceptors, given a coevolutionary relationship through sexual selection.

Evolutionary origins and dynamics of IUV

A single, deep evolutionary origin receives strong support among the 48 models tested using sex-specific scoring referred to as mutual ornamentation. IUV is lost in females early in Coliadinae and Pierinae, with multiple atavistic gains and losses throughout the diversification of these lineages. We anticipated hidden rate models to command a larger portion

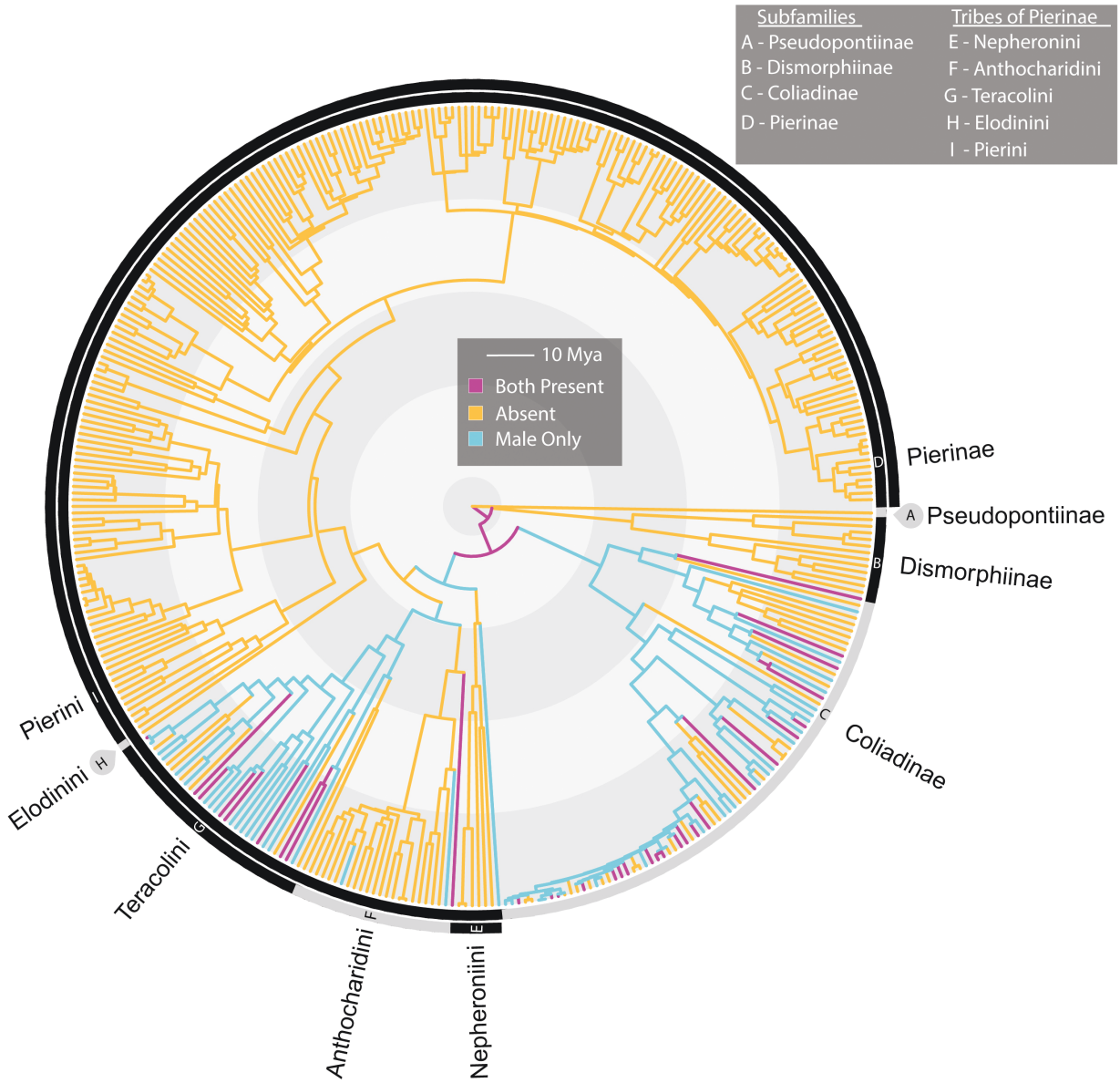

Figure 4. Best mutual ornamentation model suggests a single evolutionary origin of mutual ornamentation at the root. This model was produced using binary coding and fixing the third node joining Coliadinae and Pierinae as presence for mutual IUV (*binary.ER.F3*, see Table 1). After evolving once, IUV was subsequently lost and atavistically gained multiple times.

Table 2. Rate estimates for the binary.ER.fix3 model, showing rates of transition between absence of UV reflectance (0), male ornamentation (1), and mutual ornamentation (2).

binary.ER.F3	(1,R1)	(2,R1)	(3,R1)
(1,R1)	NA	0.01228963	NA
(2,R1)	0.01228963	NA	0.01228963
(3,R1)	NA	0.01228963	NA

of the model space due to their use in compensating for multiple underlying effects outside of the scored trait space, and though these models allow for evolutionary regimes to vary across a phylogeny (Zanne et al., 2014), they were unsuitable for our data set. Instead, the highest scoring model (binary.ER.fix3) is an equal rate model (AICw = 0.93) with very strong support. This model encoded sexually dimorphic IUV traits with binary coding and fixed the node joining Coliadinae and Pierinae as "mutually present" (presence in males and females). This estimation suggests IUV scales are homologous structures that evolved during the early history of Pieridae.

Sexual traits are theorized to evolve at faster rates than nonsexual traits (Gonzalez-Voyer & Kolm, 2011) and can drive speciation (Maan & Seehausen, 2011). It follows that a high number of transitions between trait states is common for a sexual ornament and may be due to the emergence of underlying evolvability that imparts a high level of variability in form and function (Badyaev, 2007). Impacts on variability may also be due to the interplay between sexual and ecological selection (Heinen-Kay et al., 2015), given the impacts on conspicuity for a variety of predators across different environments (Fowler-Finn & Hebets, 2011). Lande (1981) discussed the possibility of evolutionary oscillations towards and away from the equilibria between female preference and

male ornamentation. Lande's insight is observed, especially in the estimated evolutionary dynamics of the *Colias* generic radiation, where it loses and gains IUV in a pattern consistent with Lande's discussion.

Conclusions

We present two complementary analyses of IUV scales supporting a hypothesis of homology and a single early origin of IUV in Pieridae. Of 50 models tested, a single origin is strongly supported (AICcw = 0.93), suggesting intricate scale morphology that reflects iridized, ultraviolet wavelengths is as old as Pieridae and evolved once as opposed to multiple origins in a convergently evolved scenario. First, morphological comparisons of IUV scales show that IUV is always produced by stacked ridges that comprise the intricate ultrastructures on the upper laminal surface. An ANOVA of ridge density between cover and ground scales shows significant morphological differences between the scale layers. SEM revealed the consistency of the flanged lamellar ridge stacks across 11 representative species from different genera as well as a consistent lack of IUV scales in the ground-scale layer. Second, ancestral state reconstructions of IUV estimate a single early origin with repeated losses and gains. This evolutionary trajectory of IUV, which polyphyletically maps to the phylogeny, is consistent with theory on the evolution of male sexual ornaments where high diversity, both inter- and intraspecifically and including variability on IUV patterns and whether it is present or absent altogether, is predicted (Lande, 1981). Together, these analyses provide evidence that IUV patterns have an early origin in Pieridae and colors generated by structural modifications to scale morphology also evolved early in these butterflies. Our results suggest that this complex interplay results in rapid evolutionary dynamics seen in the polyphyletic distribution of the trait in the phylogeny. Future work should focus on when and how the effects of natural and sexual selection are synergistic or antagonistic in driving gain and loss across taxa given the robust body of recent literature demonstrating ecological, geographic, and sexual effects on inter- and intraspecific variation in IUV signaling for pierids.

Supplementary material

Supplementary material is available online at *Evolution*.

Data availability

Custom R scripts were then used to identify minor groups, redundant subspecies, and nonspecific taxa, which were excluded and can be found in the Dryad repository: DOI: 10.5061/dryad.8931zcrx3.

Author contributions

V.F., A.M., and R.A.P. planned the study, R.A.P. constructed phylogenies, R.A.P. and V.F. produced ancestral state reconstructions, V.F. and A.M. photographed specimens, V.F. performed SEM work and analysis of scales, V.F. wrote the manuscript, and A.M., B.A.C., R.A.P. provided edits and insight to manuscript.

Conflict of interest: The authors declare no conflict of interest.

Acknowledgments

Thanks to Robert Robbins (SNMNH) and Andrei Sourakov (FLMNH) for access to collections; Christine Brantner and Anastas Popratiloff for guidance on SEM imaging; Geoff Hill and Paweł Podkowa for access to and instruction on spectrophotometry; Cee Nell for proof-reading code; DEB-1441719 to R.A.Pyron.

References

Allyn, A. C., & Downey, J. C. (1977). Observations o nmale u-v reflectance and scale ultrastructure in Phoebis (Pieriedae). *Allyn Museum of Entomology*, 1–20.

Andersson, M., & Iwasa, Y. (1996). Sexual selection. *TREE*, *11*(2), 53–58. https://doi.org/10.1016/0169-5347(96)81042-1

Anisimova, M., & Gascuel, O. (2006). Approximate likelihood-ratio test for branches: A fast, accurate, and powerful alternative. *Systematic Biology*, *55*(4), 539–552. https://doi.org/10.1080/10635150600755453

Bates, D., Mächler, M., Bolker, B., & Walker, S. (2015). Fitting linear mixed-effects models using lme4. *Journal of Statistical Software*, *67*(1), 1–48. https://doi.org/10.18637/jss.v067.i01

Badyaev, A. V. (2007). Evolvability and robustness in color displays: Bridging the gap between theory and data.*Evolutionary Biology*, *34*, 61–71.

Beaulieu, J. M., O'Meara, B. C., & Donoghue, M. J. (2013). Identifying hidden rate changes in the evolution of a binary morphological character: The evolution of plant habit in Campanulid angiosperms. *Systematic Biology*, *62*(5), 725–737. https://doi.org/10.1093/sysbio/syt034

Beaulieu, J. M., O'Meara, B., Oliver, J., & Boyko, J. (2017). *Package "corHMM" Analysis of Binary Character Evolution.*.

Blagotić, A., & Daróczi, G. (2022). *Rapport: A report templating system* (1.1) [R]. https://cran.r-project.org/package=rapport

Blaimer, B. B., Mawdsley, J. R., & Brady, S. G. (2018). Multiple origins of sexual dichromatism and aposematism within large carpenter bees. *Evolution*, *72*(9), 1874–1889. https://doi.org/10.1111/evo.13558

Brunton, C. F. (1998). The evolution of ultraviolet patterns in European *Colias* butterflies (Lepidoptera, Pieridae): A phylogeny using mitochondrial DNA. *Heredity*, *80*(5), 611–616.

Brunton, C. F. A., & Majerus, M. E. N. (1995). Ultraviolet colours in butterflies: Intra- or inter-specific communication? *Proceedings of the Royal Society B: Biological Sciences*, *260*(1358), 199–204.

Chittka, L., & Menzel, R. (1992). The evolutionary adaptation of flower colours and the insect pollinators' colour vision. *Journal of Comparative Physiology A*, *171*(2), 171–181.

Cotton, S., Fowler, K., & Pomiankowski, A. (2004). Condition dependence of sexual ornament size and variation in the stalk-eyed fly Cyrtodiopsis Dalmanni (Diptera: Diopsidae). *Evolution*, *58*(5), 1038–1046. https://doi.org/10.1111/j.0014-3820.2004.tb00437.x

Cuthill, I. C., Partridge, J. C., Bennett, A. T., Church, S. C., Hart, N. S., & Hunt, S. (2000). Ultraviolet vision in birds. In *Advances in the study of behavior* (Vol. *29*, pp. 159–214). Academic Press.

Dapporto, L., Cini, A., Menchetti, M., Vodă, R., Bonelli, S., Casacci, L. P., Dincă, V., Scalercio, S., Hinojosa, J. C., Biermann, H., Forbicioni, L., Mazzantini, U., Venturi, L., Zanichelli, F., Balletto, E., Shreeve, T. G., Dennis, R. L. H., & Vila, R. (2017). Rise and fall of island butterfly diversity: Understanding genetic differentiation and extinction in a highly diverse archipelago. *Diversity and Distributions*, *23*(10), 1169–1181. https://doi.org/10.1111/ddi.12610

Dequeiroz, A., & Gatesy, J. (2007). The supermatrix approach to systematics. *Trends in Ecology & Evolution*, *22*(1), 34–41. https://doi.org/10.1016/j.tree.2006.10.002

Descimon, H. (1975). *Biology of pigmentation in Pieridae butterflies*. In Chemistry and Biology of Pteridines and Folates. Proceedings of the 12th International Symposium on Pteridines. De Gruyter.

Dincă, V., Zakharov, E. V., Hebert, P. D. N., & Vila, R. (2011). Complete DNA barcode reference library for a country's butterfly fauna reveals high performance for temperate Europe. *Proceedings of the Royal Society B: Biological Sciences*, *278*(1704), 347–355. https://doi.org/10.1098/rspb.2010.1089

Ding, C., & Zhang, Y. (2017). Phylogenetic relationships of Pieridae (Lepidoptera: Papilionoidea) in China based on seven gene fragments: Phylogenetic relationships of Pieridae. *Entomological Science*, *20*(1), 15–23. https://doi.org/10.1111/ens.12214

Dinwiddie, A., Null, R., Pizzano, M., Chuong, L., Leigh Krup, A., Ee Tan, H., & Patel, N. H. (2014). Dynamics of F-actin prefigure the structure of butterfly wing scales. *Developmental Biology*, *392*(2), 404–418. https://doi.org/10.1016/j.ydbio.2014.06.005

Eastman, J. M., Harmon, L. J., & Tank, D. C. (2013). Congruification: Support for time scaling large phylogenetic trees. *Methods in Ecology and Evolution*, *4*(7), 688–691. https://doi.org/10.1111/2041-210x.12051

Edger, P. P., Heidel-Fischer, H. M., Bekaert, M., Rota, J., Glöckner, G., Platts, A. E., Heckel, D. G., Der, J. P., Wafula, E. K., Tang, M., Hofberger, J. A., Smithson, A., Hall, J. C., Blanchette, M., Bureau, T. E., Wright, S. I., dePamphilis, C. W., Eric Schranz, M., Barker, M. S., … Wheat, C. W. (2015). The butterfly plant arms-race escalated by gene and genome duplications. *Proceedings of the National Academy of Sciences of the United States of America*, *112*(27), 8362–8366. https://doi.org/10.1073/pnas.1503926112

Espeland, M., Breinholt, J., Willmott, K. R., Warren, A. D., Vila, R., Toussaint, E. F. A., Maunsell, S. C., Aduse-Poku, K., Talavera, G., Eastwood, R., Jarzyna, M. A., Guralnick, R., Lohman, D. J., Pierce, N. E., & Kawahara, A. Y. (2018). A comprehensive and dated phylogenomic analysis of butterflies. *Current Biology: CB*, *28*(5), 770–778.e5. https://doi.org/10.1016/j.cub.2018.01.061

Fenner, J., Rodriguez-Caro, L., & Counterman, B. (2019). Plasticity and divergence in ultraviolet reflecting structures on Dogface butterfly wings. *Arthropod Structure & Development*, *51*, 14–22. https://doi.org/10.1016/j.asd.2019.06.001

Ficarrotta, V., Hanly, J. J., Loh, L. S., Francescutti, C. M., Ren, A., Tunström, K., Wheat, C. W., Porter, A. H., Counterman, B. A., & Martin, A. (2022). A genetic switch for male UV iridescence in an incipient species pair of sulphur butterflies. *Proceedings of the National Academy of Sciences of the United States of America*, *119*(3), e2109255118. https://doi.org/10.1073/pnas.2109255118

Fisher, R. A. (1915). The evolution of sexual preference. *The Eugenics Review*, *7*(3), 184–192.

Fowler-Finn, K. D., & Hebets, E. A. (2011). The degree of response to increased predation risk corresponds to male secondary sexual traits. *Behavioral Ecology*, *22*(2), 268–275. https://doi.org/10.1093/beheco/arq197

Ghiradella, H. (1974). Development of ultraviolet-reflecting butterfly scales: How to make an interference filter. *Journal of Morphology*, *142*(4), 395–409. https://doi.org/10.1002/jmor.1051420404

Ghiradella, H. (1984). Structure of iridescent lepidopteran scales: Variations on several themes. *Annals of the Entomological Society of America*, *77*(6), 637–645. https://doi.org/10.1093/aesa/77.6.637

Ghiradella, H., Aneshansley, D., Eisner, T., Silberglied, R. E., & Hinton, H. E. (1972). Ultraviolet reflection of a male butterfly: Interference color caused by thin-layer elaboration of wing scales. *Science*, *178*(4066), 1214–1217. https://doi.org/10.1126/science.178.4066.1214

Gonzalez-Voyer, A., & Kolm, N. (2011). Rates of phenotypic evolution of ecological characters and sexual traits during the Tanganyikan cichlid adaptive radiation. *Journal of Evolutionary Biology*, *24*(11), 2378–2388. https://doi.org/10.1111/j.1420-9101.2011.02365.x

Heidel-Fischer, H. M., Vogel, H., Heckel, D. G., & Wheat, C. W. (2010). Microevolutionary dynamics of a macroevolutionary key innovation in a Lepidopteran herbivore. *BMC Evolutionary Biology*, *10*(1), 60. https://doi.org/10.1186/1471-2148-10-60

Heinen-Kay, J. L., Morris, K. E., Ryan, N. A., Byerley, S. L., Venezia, R. E., Peterson, M. N., & Langerhans, R. B. (2015). A trade-off between natural and sexual selection underlies diversification of a sexual signal. *Behavioral Ecology*, *26*(2), 533–542. https://doi.org/10.1093/beheco/aru228

Hendry, C. R., Guiher, T. J., & Pyron, R. A. (2014). Ecological divergence and sexual selection drive sexual size dimorphism in New World pitvipers (Serpentes: Viperidae). *Journal of Evolutionary Biology*, *27*(4), 760–771. https://doi.org/10.1111/jeb.12349

Hill, J., Rastas, P., Hornett, E. A., Neethiraj, R., Clark, N., Morehouse, N., de la Paz Celorio-Mancera, M., Cols, J. C., Dircksen, H., Meslin, C., Keehnen, N., Pruisscher, P., Sikkink, K., Vives, M., Vogel, H., Wiklund, C., Woronik, A., Boggs, C. L., Nylin, S., & Wheat, C. W. (2019). Unprecedented reorganization of holocentric chromosomes provides insights into the enigma of lepidopteran chromosome evolution. *Science Advances*, *5*(6), eaau3648. https://doi.org/10.1126/sciadv.aau3648

Hirata, K., & Kubota, T. (1957). Microstructure of the scale of the butterfly, *Colias erate* poliographus Motschulsky, elucidated by electron microscopy. *Science Reports of the Kagoshima University*, *6*, 151–167.

Holmes, R. T., Schultz, J. C., & Nothnagle, P. (1979). Bird predation on forest insects: An exclosure experiment. *Science*, *206*(4417), 462–463. https://doi.org/10.1126/science.206.4417.462

Ingram, A. L., & Parker, A. R. (2008). A review of the diversity and evolution of photonic structures in butterflies, incorporating the work of John Huxley (The Natural History Museum, London from 1961 to 1990). *Philosophical Transactions of the Royal Society of London, Series B: Biological Sciences*, *363*(1502), 2465–2480. https://doi.org/10.1098/rstb.2007.2258

Kawahara, A. Y., Storer, C., Carvalho, A. P. S., Plotkin, D. M., Condamine, F. L., Braga, M. P., Ellis, E. A., St Laurent, R. A., Li, X., Barve, V., Cai, L., Earl, C., Frandsen, P. B., Owens, H. L., Valencia-Montoya, W., Aduse-Poku, K., Toussaint, E. F. A., Dexter, K. M., Doleck, T., … Nguyen, Y. -L. (2023). A global phylogeny of butterflies reveals their evolutionary history, ancestral hosts and biogeographic origins. *Nature Ecology & Evolution*, *7*, 903–913. https://doi.org/10.1038/s41559-023-02041-9

Kemp, D. J. (2008). Female mating biases for bright ultraviolet iridescence in the butterfly *Eurema hecabe* (Pieridae). *Behavioral Ecology*, *19*(1), 1–8. https://doi.org/10.1093/beheco/arm094

Kemp, D. J., & Rutowski, R. L. (2007). Condition dependence, quantitative genetics, and the potential signal content of iridescent ultraviolet butterfly coloration. *Evolution*, *61*(1), 168–183. https://doi.org/10.1111/j.1558-5646.2007.00014.x

Kemp, D. J., & Rutowski, R. L. (2011). The role of coloration in mate choice and sexual interactions in butterflies. In *Advances in the study of behavior* (Vol. *43*, pp. *55*–92). Elsevier. https://doi.org/10.1016/B978-0-12-380896-7.00002-2

Kemp, D. J., Rutowski, R. L., & Mendoza, M. (2005). Colour pattern evolution in butterflies: A phylogenetic analysis of structural ultraviolet and melanic markings in North American sulphurs. *Evolutionary Ecology Research*, *7*, 133–141.

Lande, R. (1981). Models of speciation by sexual selection on polygenic traits. *Proceedings of the National Academy of Sciences of the United States of America*, *78*(6), 3721–3725. https://doi.org/10.1073/pnas.78.6.3721

Lee, W. -S., Metcalfe, N. B., Réale, D., & Peres-Neto, P. R. (2014). Early growth trajectories affect sexual responsiveness. *Proceedings of the Royal Society B: Biological Sciences*, *281*(1777), 20132899. https://doi.org/10.1098/rspb.2013.2899

Maan, M. E., & Seehausen, O. (2011). Ecology, sexual selection and speciation. *Ecology Letters*, *14*(6), 591–602. https://doi.org/10.1111/j.1461-0248.2011.01606.x

Mazokhin-Porshnyakov, G. (1954). Ultraviolet radiation of the sun as a factor in insect habitats. *Zhurnal Obshchei Biologii*, *15*, 362–367.

McMahon, M. M., & Sanderson, M. J. (2006). Phylogenetic supermatrix analysis of GenBank sequences from 2228 papilionoid legumes. *Systematic Biology*, *55*(5), 818–836. https://doi.org/10.1080/10635150600999150

Nazari, V., Larsen, T. B., Lees, D. C., Brattström, O., Bouyer, T., Van de Poel, G., & Hebert, P. D. N. (2011). Phylogenetic systematics of

Colotis and associated genera (Lepidoptera: Pieridae): Eolutionary and taxonomic implications: Phylogenetic systematics of *Colotis*. *Journal of Zoological Systematics and Evolutionary Research*, *49*(3), 204–215. https://doi.org/10.1111/j.1439-0469.2011.00620.x

Nekrutenko, Y. P. (1965). "Gynandromorphic" effect and the optical nature of hidden wing pattern in *Gonepteryx rahmni* L. (Lepidoptera, Pieridae). *Nature*, *205*(4969), 417–418. https://doi.org/10.1038/205417a0

Ohlsson, T., Smith, H. G., Råberg, L., & Hasselquist, D. (2002). Pheasant sexual ornaments reflect nutritional conditions during early growth. *Proceedings of the Royal Society B: Biological Sciences*, *269*(1486), 21–27. https://doi.org/10.1098/rspb.2001.1848

Osorio, D. (2019). The evolutionary ecology of bird and reptile photoreceptor spectral sensitivities. *Current Opinion in Behavioral Sciences*, *30*, 223–227. https://doi.org/10.1016/j.cobeha.2019.10.009

Pagel, M. (1994). Detecting correlated evolution on phylogenies: A general method for the comparative analysis of discrete characters. *Proceedings of the Royal Society of London, Series B: Biological Sciences*, *255*(1342), 37–45. https://doi.org/10.1098/rspb.1994.0006

Paradis, E., & Schliep, K. (2019). ape 5.0: An environment for modern phylogenetics and evolutionary analyses in R. *Bioinformatics*, *35*(3), 526–528. https://doi.org/10.1093/bioinformatics/bty633

Pecháček, P., Stella, D., Keil, P., & Kleisner, K. (2014). Environmental effects on the shape variation of male ultraviolet patterns in the Brimstone butterfly (*Gonepteryx rhamni*, Pieridae, Lepidoptera). *Naturwissenschaften*, *101*(12), 1055–1063. https://doi.org/10.1007/s00114-014-1244-5

Pecháček, P., Stella, D., & Kleisner, K. (2019). A morphometric analysis of environmental dependences between ultraviolet patches and wing venation patterns in *Gonepteryx* butterflies (Lepidoptera, Pieridae). *Evolutionary Ecology*, *33*(1), 89–110. https://doi.org/10.1007/s10682-019-09969-0

Pennell, M. W., Eastman, J. M., Slater, G. J., Brown, J. W., Uyeda, J. C., FitzJohn, R. G., Alfaro, M. E., & Harmon, L. J. (2014). geiger v2.0: An expanded suite of methods for fitting macroevolutionary models to phylogenetic trees. *Bioinformatics*, *30*(15), 2216–2218. https://doi.org/10.1093/bioinformatics/btu181

Price, M. N., Dehal, P. S., & Arkin, A. P. (2010). FastTree 2—Approximately maximum-likelihood trees for large alignments. *PLoS One*, *5*(3), e9490. https://doi.org/10.1371/journal.pone.0009490

Pyron, R. A., & Wiens, J. J. (2011). A large-scale phylogeny of *Amphibia* including over 2800 species, and a revised classification of extant frogs, salamanders, and caecilians. *Molecular Phylogenetics and Evolution*, *61*(2), 543–583. https://doi.org/10.1016/j.ympev.2011.06.012

R Core Team. (2022). *R: A language and environment for statistical computing* (4.2.0) [R]. R Foundation for Statistical Computing. https://www.R-project.org

Radwan, J. (2008). Maintenance of genetic variation in sexual ornaments: A review of the mechanisms. *Genetica*, *134*(1), 113–127. https://doi.org/10.1007/s10709-007-9203-0

Revell, L. J. (2012). phytools: An R package for phylogenetic comparative biology (and other things): *phytools: R package*. *Methods in Ecology and Evolution*, *3*(2), 217–223. https://doi.org/10.1111/j.2041-210x.2011.00169.x

Rutowski, R. L. (1985). Evidence for mate choice in a sulphur butterfly (*Colias eurytheme*). *Zeitschrift für Tierpsychologie*, *70*(2), 103–114. https://doi.org/10.1111/j.1439-0310.1985.tb00504.x

Rutowski, R. L., Macedonia, J. M., Kemp, D. J., & Taylor-Taft, L. (2007). Diversity in structural ultraviolet coloration among female sulphur butterflies (Coliadinae, Pieridae). *Arthropod Structure & Development*, *36*(3), 280–290. https://doi.org/10.1016/j.asd.2006.11.005

Rutowski, R. L., Macedonia, J. M., Morehouse, N., & Taylor-Taft, L. (2005). Pterin pigments amplify iridescent ultraviolet signal in males of the orange sulphur butterfly, *Colias eurytheme*. *Proceedings of the Royal Society B: Biological Sciences*, *272*(1578), 2329–2335. https://doi.org/10.1098/rspb.2005.3216

Schluter, D., Price, T., Mooers, A., & Ludwig, D. (1997). Likelihood of Ancestor states in adaptive radiation. *Evolution*, *51*(6), 1699–1711. https://doi.org/10.1111/j.1558-5646.1997.tb05095.x

Shur, V. Y., Kuznetsov, D. K., Pryakhina, V. I., Kosobokov, M. S., Zubarev, I. V., Boymuradova, S. K., & Volchetskaya, K. V. (2017). Study of structural colour of Hebomoia glaucippe butterfly wing scales. *IOP Conference Series: Materials Science and Engineering*, *256*(1), 012014. IOP Publishing.

Silberglied, R. E., & Taylor, O. R. (1973). Ultraviolet differences between the sulphur butterflies, *Colias eurytheme* and *C. philodice*, and a possible isolating mechanism. *Nature*, *241*(5389), 406–408. https://doi.org/10.1038/241406a0

Silberglied, R. E., & Taylor, O. R. (1978). Ultraviolet reflection and its behavioral role in the courtship of the sulfur butterflies *Colias eurytheme* and *C. philodice* (Lepidoptera, Pieridae). *Behavioral Ecology and Sociobiology*, *3*(3), 203–243. https://doi.org/10.1007/bf00296311

Simmons, M. P., & Goloboff, P. A. (2014). Dubious resolution and support from published sparse supermatrices: The importance of thorough tree searches. *Molecular Phylogenetics and Evolution*, *78*, 334–348. https://doi.org/10.1016/j.ympev.2014.06.002

Smith, S. A., Beaulieu, J. M., & Donoghue, M. J. (2010). An uncorrelated relaxed-clock analysis suggests an earlier origin for flowering plants. *Proceedings of the National Academy of Sciences of the United States of America*, *107*(13), 5897–5902. https://doi.org/10.1073/pnas.1001225107

Smith, S. A., & O'Meara, B. C. (2012). treePL: Divergence time estimation using penalized likelihood for large phylogenies. *Bioinformatics*, *28*(20), 2689–2690. https://doi.org/10.1093/bioinformatics/bts492

Smith, S. A., & Walker, J. F. (2019). Py PHLAWD: A python tool for phylogenetic dataset construction. *Methods in Ecology and Evolution*, *10*(1), 104–108. https://doi.org/10.1111/2041-210X.13096

Stamatakis, A. (2014). RAxML version 8: A tool for phylogenetic analysis and post-analysis of large phylogenies. *Bioinformatics*, *30*(9), 1312–1313. https://doi.org/10.1093/bioinformatics/btu033

Stavenga, D. G., Giraldo, M. A., & Hoenders, B. J. (2006). Reflectance and transmittance of light scattering scales stacked on the wings of pierid butterflies. *Optics Express*, *14*(11), 4880–4890. https://doi.org/10.1364/oe.14.004880

Stella, D., Faltýnek Fric, Z., Rindoš, M., Kleisner, K., & Pecháček, P. (2018). Distribution of ultraviolet ornaments in Colias butterflies (Lepidoptera: Pieridae). *Environmental Entomology*, *47*(5), 1344–1354. https://doi.org/10.1093/ee/nvy111

Stella, D., & Kleisner, K. (2022). Visible beyond violet: How butterflies manage ultraviolet. *Insects*, *13*(3), 242. https://doi.org/10.3390/insects13030242

Stella, D., Pecháček, P., Meyer-Rochow, V. B., & Kleisner, K. (2018). UV reflectance is associated with environmental conditions in Palaearctic Pieris napi (Lepidoptera: Pieridae). *Insect Science*, *25*(3), 508–518. https://doi.org/10.1111/1744-7917.12429

van der Bijl, W., Zeuss, D., Chazot, N., Tunström, K., Wahlberg, N., Wiklund, C., Fitzpatrick, J. L., & Wheat, C. W. (2020). Butterfly dichromatism primarily evolved via Darwin's, not Wallace's, model. *Evolution Letters*, *4*(6), 545–555. https://doi.org/10.1002/evl3.199

Van Der Kooi, C. J., Stavenga, D. G., Arikawa, K., Belušič, G., & Kelber, A. (2021). Evolution of insect color vision: From spectral sensitivity to visual ecology. *Annual Review of Entomology*, *66*, 435–461. https://doi.org/10.1146/annurev-ento-061720-071644

Wahlberg, N., Rota, J., Braby, M. F., Pierce, N. E., & Wheat, C. W. (2014). Revised systematics and higher classification of pierid butterflies (Lepidoptera: Pieridae) based on molecular data. *Zoologica Scripta*, *43*(6), 641–650. https://doi.org/10.1111/zsc.12075

Watt, W. B. (1964). Pteridine components of wing pigmentation in the butterfly *Colias eurytheme*. *Nature*, *201*(4926), 1326–1327.

Watt, W. B. (1967). Pteridine Biosynthesis in the butterfly *Colias eurytheme*. *The Journal of Biological Chemistry*, *242*(4), 565–572. https://doi.org/10.1016/S0021-9258(18)96242-3

Wickham, H., François, R., Henry, L., & Müller, K. (2022). *dplyr: A Grammar of Data Manipulation* (1.0.9) [R]. https://CRAN.R-project.org/package=dplyr

Wiemers, M., Chazot, N., Wheat, C. W., Schweiger, O., & Wahlberg, N. (2020). A complete time-calibrated multi-gene phylogeny of the European butterflies. *ZooKeys*, *938*, 97–124. https://doi.org/10.3897/zookeys.938.50878

Wijnen, B., Leertouwer, H. L., & Stavenga, D. G. (2007). Colors and pterin pigmentation of pierid butterfly wings. *Journal of Insect Physiology*, *53*(12), 1206–1217. https://doi.org/10.1016/j.jinsphys.2007.06.016

Wilts, B. D., Pirih, P., & Stavenga, D. G. (2011). Spectral reflectance properties of iridescent pierid butterfly wings. *Journal of Comparative Physiology. A Neuroethology, Sensory, Neural, and Behavioral Physiology*, *197*(6), 693–702. https://doi.org/10.1007/s00359-011-0632-y

Yang, Z. (2006). *Computational molecular evolution*. Oxford.

Zanne, A. E., Tank, D. C., Cornwell, W. K., Eastman, J. M., Smith, S. A., FitzJohn, R. G., McGlinn, D. J., O'Meara, B. C., Moles, A. T., Reich, P. B., Royer, D. L., Soltis, D. E., Stevens, P. F., Westoby, M., Wright, I. J., Aarssen, L., Bertin, R. I., Calaminus, A., Govaerts, R., … Beaulieu, J. M. (2014). Three keys to the radiation of angiosperms into freezing environments. *Nature*, *506*(7486), 89–92. https://doi.org/10.1038/nature12872